

ORIGINAL ARTICLE

Isoflurane Impairs Immature Astroglia Development In Vitro: The Role of Actin Cytoskeleton

Nadia Lunardi, MD, Christoph Hucklenbruch, MD, Janelle R. Latham, BS, Joseph Scarpa, and Vesna Jevtovic-Todorovic, MD, PhD, MBA

Abstract

General anesthetics, either alone or in combination, can be detrimental to the developing mammalian brain and induce extensive apoptotic degeneration of immature neurons when they are administered at the peak of synaptogenesis. Because neuron development and normal functions depend on the integrity of astroglia, we sought to determine whether general anesthesia also causes disturbances in the early development of astroglia. Using isoflurane, an inhaled anesthetic that is highly toxic to immature neurons, we studied primary astroglia cultures, focusing on very early development (Day-In-Vitro 4 treatment). Exposure to 3% isoflurane for 24 hours delayed morphological differentiation and impaired the growth of immature astrocytes. The timing of delayed astroglia maturation and growth coincided with a major disturbance in actin cytoskeleton sculpting that was manifest as impaired actin stress fiber formation and cytoskeletal organization and downregulation of the focal adhesion protein, paxillin. Isoflurane-induced actin cytoskeletal changes were accompanied by a significant decrease in protein levels of the endogenous GTPase RhoA that regulates the phosphorylation of myosin light chain protein, suggesting that isoflurane-induced impairment in glial growth and morphological development is, in part, mediated by the RhoA/myosin light chain protein signaling pathway.

Key Words: Actin, Anesthesia neurotoxicity, Astrocyte, Development, Myosin light chain, Primary culture, RhoA.

INTRODUCTION

During the last several years, we and others have demonstrated that widely used general anesthetics can damage the developing mammalian brain. A variety of such anesthetics,

including benzodiazepines, barbiturates, propofol, ketamine, and volatile anesthetics, used alone or in combination at the peak of synaptogenesis, cause widespread apoptotic neurodegeneration in vulnerable brain regions in rats, mice, guinea pigs, and nonhuman primates (1–7). Moreover, examination of the ultrastructural properties of newly formed synapses has demonstrated that anesthesia causes long-term impairment of synapse formation, manifested as significant decreases in both synapse volumetric densities and complexity. These changes are accompanied by scarcity and disarray of the neuropil (8).

Astroglia, the most abundant glial cells, control every aspect of brain development by regulating neuronal migration, maturation, and synapse sculpting (e.g. synapse number, function, and stability) (9, 10). Neurons cultured in the absence of the astrocytic feeding layer have decreased synaptic density; there is also little spontaneous synaptic activity of the existing synapses (10, 11).

Normally, astrocytes not only promote de novo formation of synapses, but also stabilize existing synapses. It seems that γ -amino butyric acid A (GABAA) receptors are expressed in astrocytes in vitro and in vivo and that GABA signaling is, at least in part, responsible for morphological changes in immature and mature astrocytes (12, 13), suggesting that modulation of GABA could influence astrocyte development and function. Because research to date on anesthesia-induced neurotoxicity has mainly focused on examining the cellular mechanisms of neuron degeneration, we postulated that the anesthesia-induced death of neurons could be associated with anesthesia-induced disturbances in astroglia development. In particular, it is important to examine whether and how general anesthetics, potent modulators of GABAA receptors (14), disturb astroglia development.

The actin cytoskeleton is the major determinant of astroglia morphology and function. Hence, understanding of glial development rests on an appreciation of the signaling pathways controlling the organization and dynamics of the actin cytoskeleton (15). Such signaling pathways are regulated by a family of small GTPases, one of the most influential of which is RhoA (16). Like other GTPases, RhoA functions as a molecular switch, cycling between an inactive GDP-bound state and an active GTP-bound state. It regulates the phosphorylation of myosin light chain proteins (MLC-P), which, in turn, promote the organization of the actin cytoskeleton in actin stress fibers (ASFs) and the formation of focal adhesions. Modulation of the RhoA signaling pathway by ethanol (the most commonly used CNS depressant and

From the Department of Anesthesiology (NL, CH, JRL, JS, VJ-T), University of Virginia, Charlottesville, Virginia; Department of Anesthesiology and Pharmacology (NL), University of Padova, Padova, Italy; and Department of Anesthesiology and Intensive Care (CH), University Hospital Muenster, Muenster, Germany.

Send correspondence and reprint requests to: Vesna Jevtovic-Todorovic, MD, PhD, Department of Anesthesiology, University of Virginia Health System, P.O. Box 800710, Charlottesville, VA 22908; E-mail: vj3w@virginia.edu

This study was supported by the National Institutes of Health/National Institute of Child Health and Human Development HD 44517 (to Vesna Jevtovic-Todorovic), John E. Fogarty Award TW007423-128322 (to Vesna Jevtovic-Todorovic), ARRA supplement NIH/NICHD HD 44517 (to Vesna Jevtovic-Todorovic), and Harold Carron endowment (to Vesna Jevtovic-Todorovic). Vesna Jevtovic-Todorovic is an established investigator of the American Heart Association.

oldest anesthetic) causes severe disruption of the actin cytoskeleton, ultimately leading to impairment of astrocyte morphological differentiation and function (17, 18).

To begin to understand whether and how anesthetics affect astroglia development, we exposed immature primary astroglia cultures to the inhalational anesthetic isoflurane and studied its effect on astroglia maturation and sculpting of actin cytoskeleton. This *in vitro* model enabled us to examine astroglia during their transformation from radial (i.e. very immature) glia to more mature astrocytes and to study them in isolation without the interference of anesthesia effects on the developing neurons, which is not possible to accomplish using *in vivo* models.

MATERIALS AND METHODS

Astroglia Cultures

Primary cultures of astrocytes from 1- to 2-day-old Sprague-Dawley rat pups were prepared as described (19). Brain tissue was freed from meninges and dissected by removing the cerebellum, olfactory bulb, and brainstem; this tissue was minced under sterile conditions. The cell suspension was made with Hank's balanced salt solution and 4-(2-hydroxyethyl)-1-piperazineethanesulfonic acid buffers (Gibco BRL, Carlsbad, CA) and treated with 1% DNase (Sigma, St. Louis, MO) and 2.5% trypsin (Gibco BRL). After centrifuging at 800 rpm for 5 minutes, the pellet was resuspended in culture medium (Minimum Essential Medium with Earle's salts) containing 10% horse serum (Gibco BRL), 6% glucose, and penicillin-streptomycin (Gibco BRL). The day of plating was designated as Day-In-Vitro 0 (DIV0). Cultures were grown in an incubator in a constant humidified atmosphere of 5% carbon dioxide and 95% air at 37°C. Medium was changed the day after plating (DIV1) and every third day thereafter. The plated cell density was approximately 50,000 cells/dish (Fluorodish FD35-100; World Precision Instruments Inc., Sarasota, FL). We used 35-mm glass-bottom dishes that had been treated with poly-L-lysine (Sigma) 2 to 3 days before plating. The purity of astrocyte cultures was assessed by immunofluorescence using a mouse anti-glial fibrillary acidic protein (GFAP) monoclonal antibody. Possible contamination by neurons was assessed using an anti-microtubule-associated protein 2 antibody and found to be about 1%. Under our conditions, 95% of the cells were astrocytes. This culturing method provides astrocyte-enriched cultures with microglia contamination approximately 4% (20, 21).

Because the plating density of immature glia (and thus their ability to touch and connect) is a crucial determinant of growth and morphological development, we prescreened all culture dishes on DIV4 immediately before treatment and selected only dishes with relatively uniformly distributed cells of low density (40–80 cells/mm²). The accuracy of prescreening was confirmed by randomly selecting approximately 10% of dishes from the same batch. These were then stained and analyzed as outlined below. The plating density resulted in confluent monolayers of astrocytes in 10 to 14 days. At preselection, culture dishes were randomly assigned to control and experimental groups.

Isoflurane Treatment

Primary astrocyte cultures were exposed to isoflurane for 24 hours either at DIV4 (very immature) or DIV15 (more mature). Treatment was done at 37°C in a humidified atmosphere containing 3% isoflurane, 5% carbon dioxide, and 92% air (experimental dishes) using a specially designed gas chamber that allowed a constant flow of isoflurane. This concentration of isoflurane (administered at 3.4%) has been shown to be clinically relevant for the treatment of primary rat neuronal cultures (22). This procedure is based on *in vivo* studies in which the inspired minimum alveolar concentration of isoflurane required to achieve a surgical plane of anesthesia in immature rat pups was determined to be 3.6% to 4% (23). It is noteworthy that the minimum alveolar concentration requirement for isoflurane in immature rat pups is about 2 times higher than that required by adult animals. Thus, the resulting free concentration of 3% isoflurane in culture medium at 37°C (determined to be ~0.7 mmol/L [24]) could be considered clinically relevant in this age population. Sham control dishes were kept in the same atmosphere but in the absence of isoflurane. The chamber design enabled the gas composition to which culture dishes were exposed to be analyzed continuously using an infrared analyzer (Datex Ultima, Chalfont, St. Giles, United Kingdom). After 24 hours, the dishes were taken out of the anesthesia chamber and immediately placed in an incubator. True control dishes were kept in the incubator and were not exposed to any treatment.

Western Blotting and Immunoprecipitation

Astroglia from sham control and isoflurane-treated dishes were collected at various DIV with a cell scraper, lysed in 100 μ L of lysis buffer (RIPA Buffer; Thermo Scientific, Rockford, IL) per dish and 10 μ L of protease inhibitors (Sigma) per dish, and then centrifuged at 14,000 rpm for 15 minutes at 4°C. The supernatant was then collected, mixed with sample buffer (2 \times Laemmli Sample Buffer; Sigma), and boiled at 90°C to 100°C for 5 minutes. Although *in vivo* vimentin protein expression steadily declines until Postnatal Day 21, *in vitro* vimentin protein expression in primary rat glia during the first 15 days after plating does not change significantly (25, 26). Therefore, vimentin was used as an internal loading control for total actin, GFAP, RhoA, and paxillin measurements. Equal amounts of proteins (5–10 μ g) were electrophoresed on sodium dodecyl sulfate–polyacrylamide gel electrophoresis gels (8% for actin and RhoA, 10% for paxillin, GFAP, vimentin, and MLC-P) and then transferred to nitrocellulose membranes. The primary antibodies used were anti-RhoA monoclonal antibody (1:50; Santa Cruz Biotechnologies, Santa Cruz, CA), anti-paxillin monoclonal antibody (1:75; Transduction Laboratories, San Jose, CA), anti-vimentin monoclonal antibody (1:100; Sigma), anti-GFAP monoclonal antibody (1:2500; DakoCytomation, Glostrup, Denmark), and anti-p-MYL9 (myosin light chain, Thr18/Ser19) polyclonal antibody (1:100; Santa Cruz Biotechnology). Membranes were exposed to antibodies diluted in Tris buffered saline–Tween 0.1% overnight. The secondary antibodies used were HRP-conjugated anti-mouse immunoglobulin G for RhoA, paxillin, and vimentin (1:5000); HRP-conjugated anti-rabbit for GFAP (1:8000); and horseradish peroxidase–conjugated anti-goat for

MLC-P diluted in Tris buffered saline–Tween 0.1% for 1 hour. Membranes were developed using the enhanced chemiluminescence system (ECL Plus; Amersham, Arlington Heights, IL). When needed, membranes were washed in Restore Western Blot Stripping Buffer (Thermo Scientific) for 7.5 minutes at 37°C. Gels were scanned with a Bio-Rad GS-800 Densitometer and quantified using Image Quant TL 2005.

For immunoprecipitation studies (total MLC and MLC-P), lysates were precleared by the addition of 1 µg of goat immunoglobulin G (sc-2028; Santa Cruz Biotechnology) with 20 µL A/G Plus-Agarose (Santa Cruz Biotechnology), followed by incubation for 1 hour with anti-p-MYL9 antibodies and protein A/G Plus agarose beads. To detect MLC and MLC-P, 25 µg of total cell proteins were immunoprecipitated using 10 µL of anti-MYL9 antibodies. Western blot was then performed as described.

Morphological Studies

Sham control and isoflurane-treated primary astrocytic cultures were followed from DIV4 until DIV15. On DIV posttreatment, the cells were washed in PBS, fixed with freshly prepared paraformaldehyde (4% in PBS) at room temperature for 20 minutes, and permeabilized for 15 minutes in Triton-X 0.1% in PBS. Cells were then incubated with 1% 4',6-diamidino-2-phenylindole (DAPI) stain (D1306; Invitrogen, Carlsbad, CA) for 25 minutes at room temperature, followed by phalloidin stain (1:40; Oregon Green 514 Phalloidin, Invitrogen). After rinsing, the cells were examined by light microscopy (Nikon Eclipse TE200). For analysis, 5 random nonoverlapping photographs were taken per dish.

Growth Studies

We followed the growth rates of cultured astrocytes starting from either DIV4 or DIV15 (immediately before treatment) and daily thereafter. After staining the dishes with DAPI, 5 random nonoverlapping pictures were taken of a known area per dish (total 15–33 dishes per time point per litter; 8 litters used). Every DAPI-stained nucleus was counted as 1 cell. The number of nuclei per picture was obtained using ImageJ software (NIH Image, Bethesda, MA). The total number of cells per dish, expressed as number of cells per square millimeter, was derived as the average of the nuclei counted in each of the 5 pictures. To assess whether the DAPI-stained cells were alive, randomly selected dishes were double stained with a live/dead viability/cytotoxicity kit for mammalian cells (Molecular Probes, Invitrogen). Bright green fluorescent cells were recorded as live cells because membrane-permeant calcein AM, which is cleaved by esterases in live cells, yields green fluorescence. Red fluorescent cells were counted as dead cells because membrane-impermeant ethidium homodimer-1, which labels the nucleic acids of membrane-compromised cells, yields red fluorescence.

Statistics

Comparisons among the groups were made using 1-way analysis of variance or Kruskal-Wallis analysis, followed when necessary by Tukey test (post hoc analysis) (GraphPad Prism, La Jolla, CA). Significance was set at $p < 0.05$.

RESULTS

Temporal Pattern of GFAP and Vimentin Expression During Maturation of Astroglia In Vitro

Several lines of evidence suggest that expression of GFAP gradually increases as astroglia mature both in vitro and in vivo (25–27), whereas changes in protein expression of vimentin differ under in vivo and in vitro conditions. In vivo vimentin protein expression in rodents decreases around Postnatal Day 7, whereas it remains relatively unchanged or slightly elevated for the first 15 days in vitro (25, 26). Therefore, whereas vimentin expression is an unreliable indicator of glial maturity, GFAP levels are often used for assessing glial maturity in vitro with very low levels typically detected in very immature glial cultures. We found minimal GFAP expression in DIV4 cultures, but a steady increase in expression at DIV7

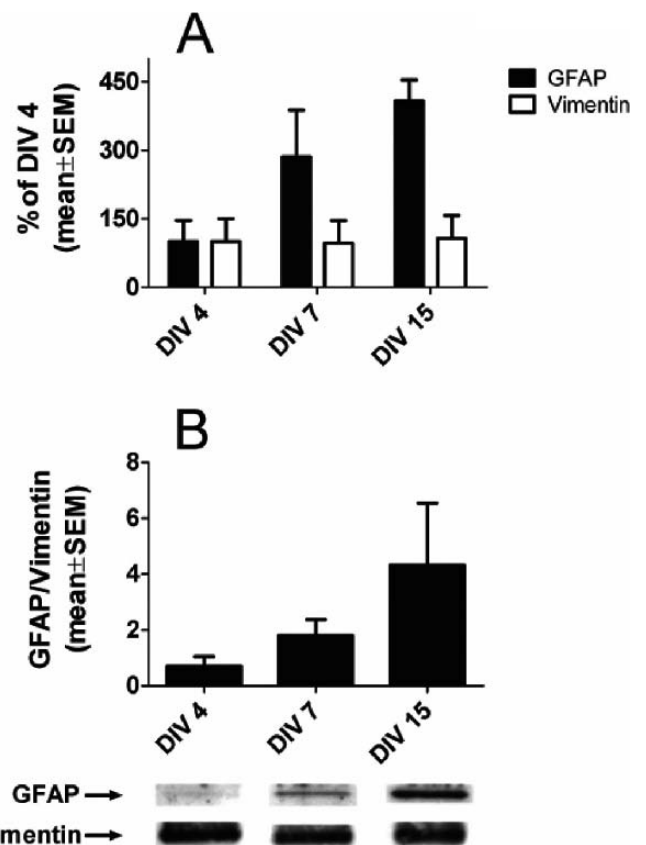


FIGURE 1. The protein content of glial fibrillary acidic protein (GFAP) increases as cultured primary astroglia mature, whereas vimentin content remains constant. **(A)** Western blot analysis of true control primary glia cultures shows that the GFAP protein contents in Day-In-Vitro 7 (DIV7) and DIV15 cultures are increased 2.8- and 4-fold, respectively, as compared with those of DIV4 cultures. Vimentin protein levels remained unchanged in DIV7 and DIV15 cultures. The values shown are means ± SEM of the densitometric analysis from 4 different primary cultures per time point. **(B)** Ratios of GFAP to vimentin densitometric values at the 3 time points. Corresponding representative Western blots are shown underneath the graphs.

and DIV15; compared with DIV4, the increases on these days were 2.8- and about 4-fold, respectively (Fig. 1A). Vimentin levels remained unchanged in DIV7 and DIV15 cultures compared with the level at DIV4 (Fig. 1B; $n = 4$ per data point). Therefore, we used DIV4 as very immature and DIV15 as more mature astroglia cultures for analysis.

Isoflurane Disrupts Morphological Transformation of Astroglia and Impairs F-Actin Organization

The regulation of astrocyte morphology is highly dependent on the actin cytoskeleton. Astrocytes in DIV4 untreated cultures displayed a spindle-like appearance, with small cell bodies, bipolar organization of the processes, and scarce actin filaments (Fig. 2A). Under sham control conditions, radial glia underwent morphological differentiation; at DIV7, this was indicated by their transformation into flat polygonal cells with fibroblast-like morphology and relatively large cell bodies, although still without any major processes elongating from them (Fig. 2B). As labeled by phalloidin, F-actin at this stage

was arranged mainly in ASF, distinct filament bundles running throughout the cytoplasm. By DIV10, astroglia became fairly confluent, with major processes elongating from the cell bodies and running on top of each other, becoming intermingled and displaying a complex architecture (Fig. 2C). F-actin gradually became more densely organized in rich, thick, parallel-running stress fibers. Astrocytes in cultures exposed to 3% isoflurane for 24 hours, although morphologically indistinguishable from the sham controls before treatment at DIV4, displayed changes indicative of delayed transformation of radial glial cells into normal fibroblast-like morphology at DIV7 (Fig. 2D). Indeed, the isoflurane-treated DIV7 astroglia seemed similar to DIV4 radial glial cells, having no morphological properties typical of flat polygonal cells and lacking organized actin filament bundles. In some cells, actin started to reorganize into groups of filaments at the cell periphery, forming cortical actin.

The transformation of astroglia into flat polygonal cells occurred at DIV10 (Fig. 2E) instead of DIV7, as in the sham controls (Fig. 2B), suggesting that there was a delay in the morphological transformation of immature glia to more mature

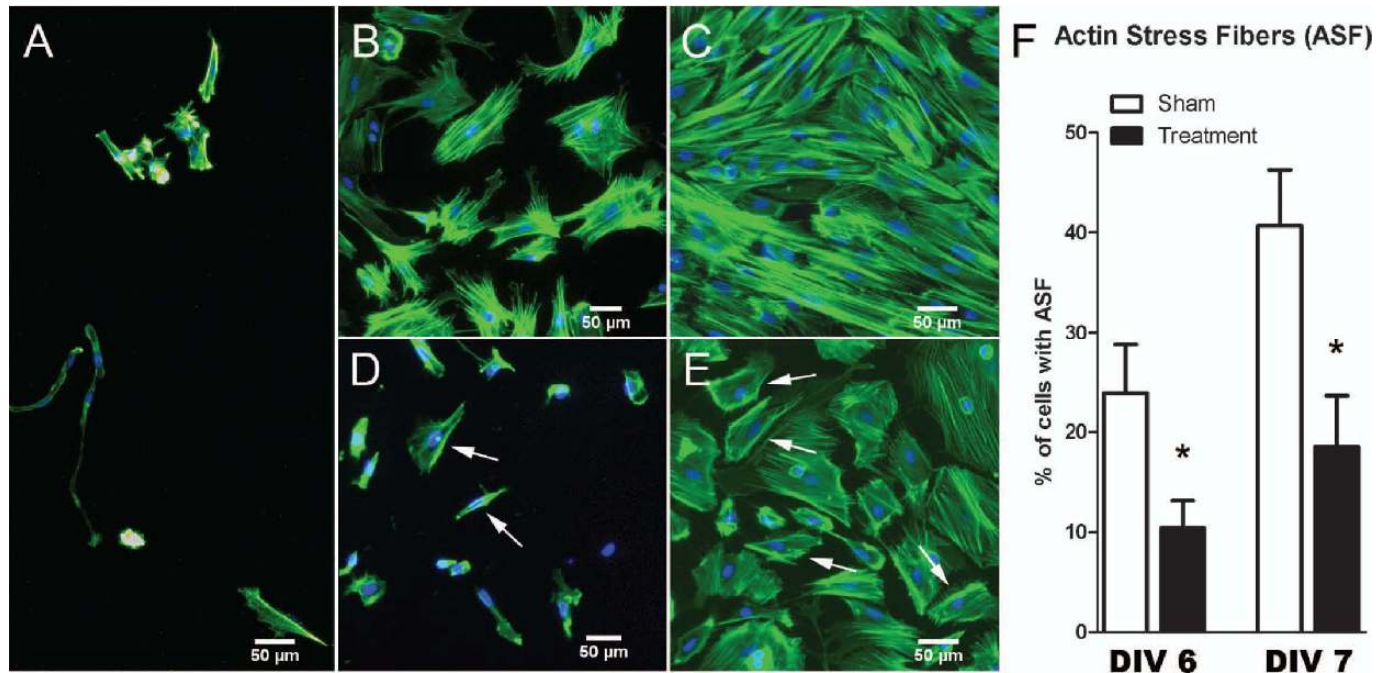


FIGURE 2. Isoflurane impairs the morphological transformation and cellular organization of cytoskeletal actin in cultured primary astroglia. **(A)** Immature astroglia at Day-In-Vitro 4 (DIV4), immediately before treatment, exhibit long thin processes extending from one or both ends of their small cell bodies. **(B, C)** Sham control astrocytes at DIV7 **(B)** and DIV10 **(C)** show progressive morphological changes indicative of maturation. At DIV7, they display fibroblast-like morphology with flat polygonal cell bodies and short stubby processes. By DIV10, their processes are longer and highly intermingled; intense growth results in the formation of a thick monolayer of cells. F-actin is arranged mainly in the actin stress fibers (ASFs). By DIV10, ASFs gradually become more densely organized in parallel stress fibers. **(D, E)** Isoflurane-treated astrocytes at DIV7 **(D)** and 10 **(E)** show delayed morphological transformation. At DIV7, they still display bipolar spindle-like shape similar to their appearance in DIV4 cultures **(A)**. Note the scarcity of cells compared with **(B)**. By DIV10, the treated astrocytes still lag behind same-age sham control cultures and display morphological features similar to those in DIV7 sham controls **(B)**. There is a lack of organized actin filament bundles. In some cells, actin has started to reorganize into groups of filaments at the cell periphery, forming cortical actin (arrows). **(A–E)** Phalloidin staining, original magnification: 10 \times . **(F)** Percentages of astroglia containing ASFs in DIV6 and DIV7 cultures treated on DIV4. There were significantly fewer cells containing organized ASFs in treated versus sham cultures. There was a 2-fold decrease in the percentage of astrocytes showing reorganization of cytoskeletal actin into ASFs on DIV6 and DIV7 (* $p < 0.05$; $n = 511$ – 639 cells per data point; sampling done on 3 cultures per data point).

ones. It is noteworthy that F-actin in isoflurane-treated cultures at DIV10 still did not seem to be as finely organized as in sham controls, with many profiles displaying cortical actin (Fig. 2E).

We assessed this phenomenon by quantifying the percentage of cells in experimental and sham control groups displaying ASF at DIV6 and DIV7 (i.e. 1 and 2 days posttreatment, respectively). As expected, we found a significant decrease in the number of astrocytes containing ASF in isoflurane-treated astroglia versus those in sham controls on both days (Fig. 2F; * $p < 0.05$; $n = 511$ – 639 cells per data point).

Isoflurane Impairs the Growth of Very Immature but Not More Mature Cultured Astroglia

To assess the effect of anesthesia on astrocyte growth in vitro, we exposed cultured astroglia at DIV4 or DIV15 to 3% isoflurane for 24 hours and followed them up to 11 days or 3 days posttreatment, respectively (Fig. 3). When treated in a very immature state at DIV4, astroglia were highly sensitive to isoflurane, as demonstrated by a significant decrease in numbers of cells versus age-matched sham controls at DIV6 and DIV7 (Fig. 3A; * $p < 0.05$). Although the difference was not statistically significant at DIV8 to DIV10 (3–5 days after treatment), the growth of experimental glia still lagged behind

that of sham controls. There was also a decrease in cell density versus age-matched sham controls that ranged from about 40% at DIV6 to about 20% to 30% from DIV7 to DIV10 (Fig. 3B).

When treated in a more mature state at DIV15, isoflurane had no significant effect on cell density during the first 3 days after treatment (Fig. 3C) when immature glia were most sensitive ($n = 19$ – 33 dishes per data point for DIV4 experiments; $n = 15$ dishes per data point for DIV15 experiments). When the numbers of dead versus live cells were assessed using a live/dead viability/cytotoxicity kit, the number of dead cells in the experimental dishes was less than 4% of the total cell density, as counted with DAPI staining, a level that was comparable to sham controls at any given posttreatment day (data not shown). Based on these results, the DIV7 (2 days post-treatment) time point was used in subsequent analyses.

Isoflurane Has No Effect on the Protein Levels of GFAP, Vimentin, and Total Actin in Immature Astroglia

To assess the effects of isoflurane on cytoskeletal proteins, we exposed cultured astroglia at DIV4 to 3% isoflurane or air for 24 hours and measured the levels of GFAP, vimentin, and actin at DIV7. There were no changes in levels of GFAP,

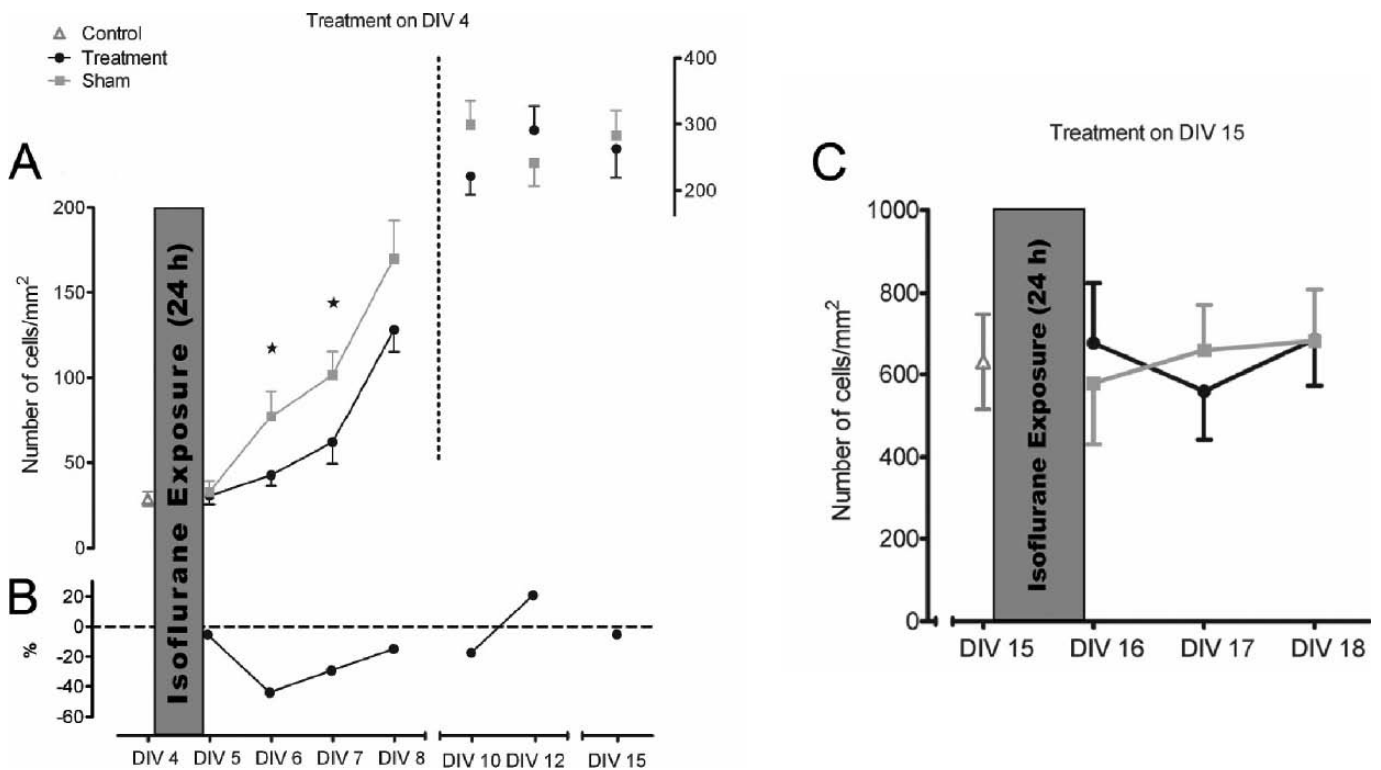
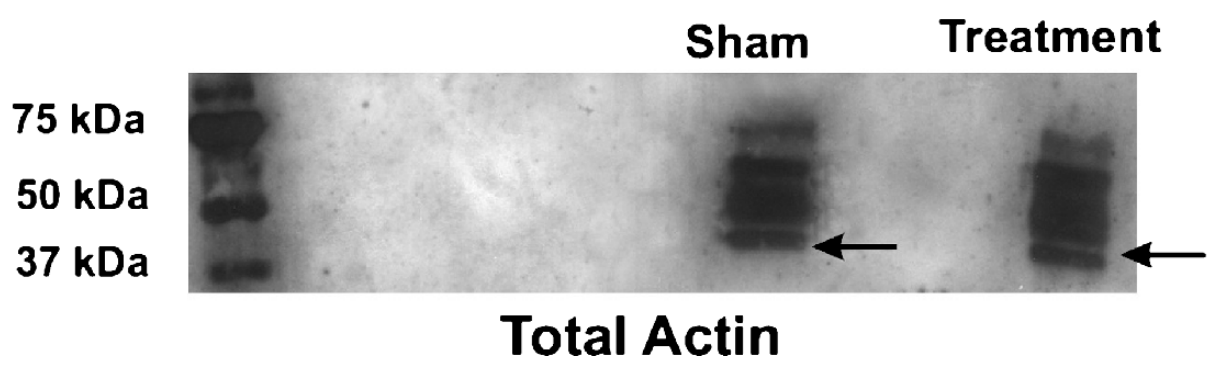
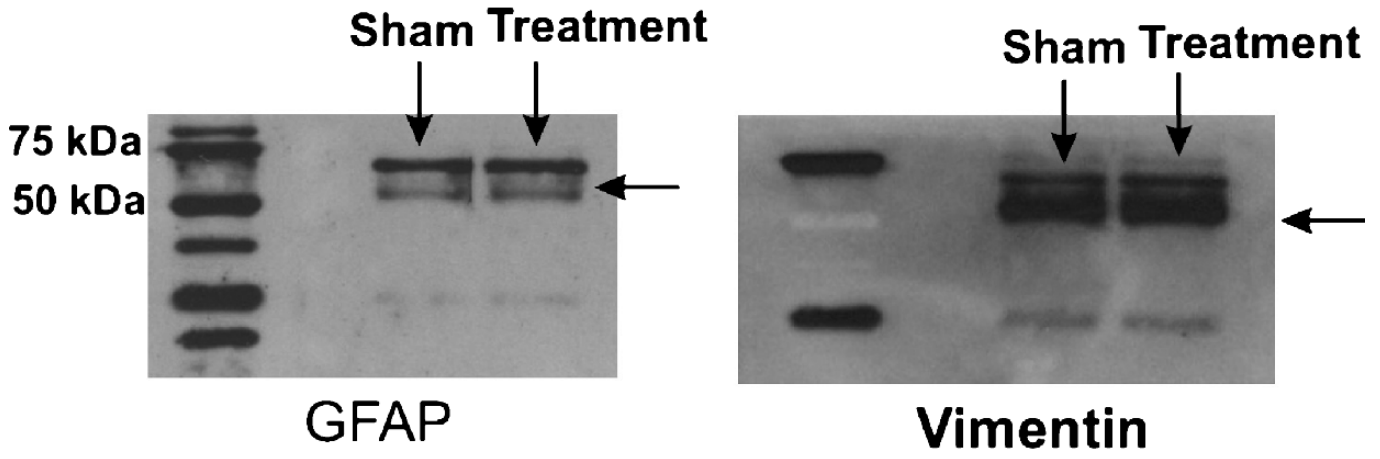
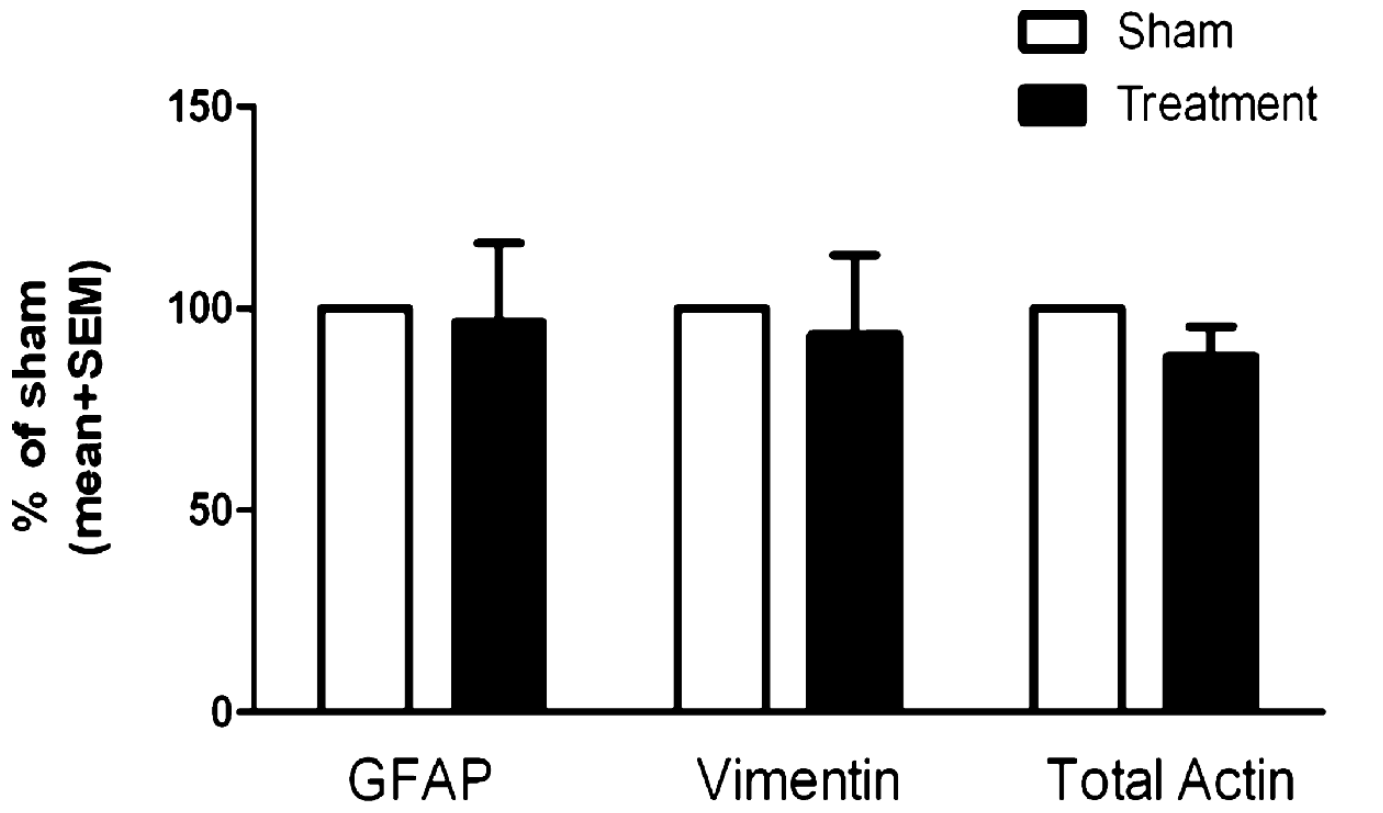


FIGURE 3. Isoflurane impairs the growth of immature but not more mature primary astroglia. **(A)** Isoflurane treatment of astroglia on Day-In-Vitro 4 (DIV4) results in a significant decrease in the number of cells at DIV6 and DIV7 (closed circles, Treatment) versus age-matched sham controls (closed squares, Sham) (* $p < 0.05$). At DIV8 to DIV10, the growth of treated glia lags behind that of sham controls, although the difference is not statistically significant. **(B)** There is a decrease in cell density compared with age-matched sham controls (dashed line, age-relevant baseline), ranging from about 40% at DIV6 to approximately 20% to 30% from DIV7 to DIV10. **(C)** Cells treated at DIV15 are resistant to isoflurane treatment ($n = 19$ – 33 dishes per data point for DIV4 experiments; $n = 15$ dishes per data point for DIV15 experiments). Cell densities immediately before treatment (DIV4) are marked with an open triangle (Control).



Downloaded from https://academic.oup.com/jnen/article/70/4/281/2917328 by guest on 16 August 2022

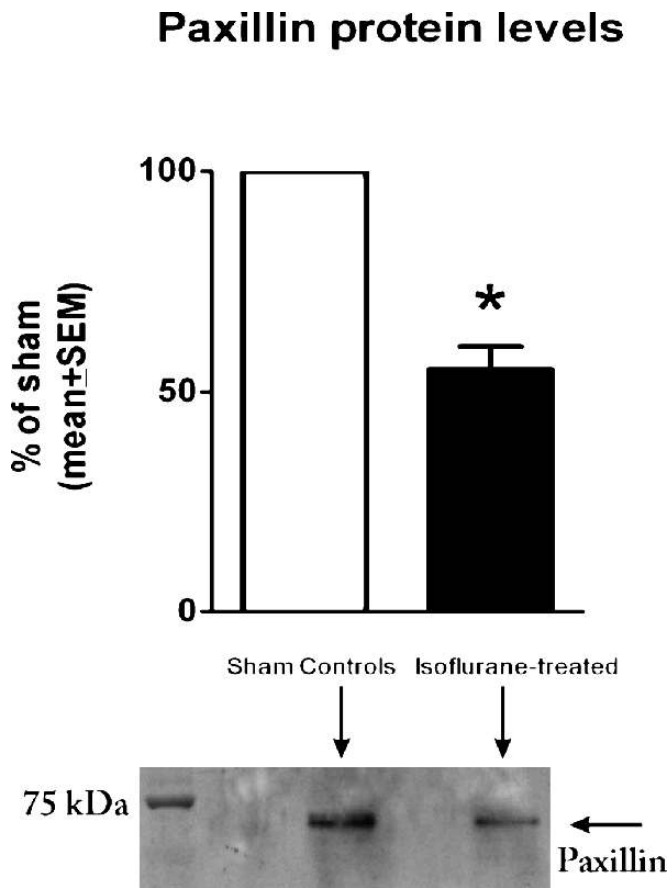


FIGURE 5. Isoflurane induces a significant decrease in protein levels of paxillin in immature primary astroglia. Isoflurane treatment at Day-In-Vitro 4 (DIV4) (3% for 24 hours) causes an approximately 50% decrease in the protein content of paxillin when measured at DIV7 (2 days posttreatment; * $p < 0.005$; $n = 4$ per data point). Experimental cultures were compared with age-matched sham control cultures (designated as 100%). Corresponding representative Western blots are shown below the graph.

vimentin, or total actin (Fig. 4). Experimental cultures were compared with age-matched sham controls (noted as 100%) ($n = 4$ per data point).

Isoflurane Decreases Protein Levels of Paxillin

We next examined whether isoflurane also affects paxillin, a focal adhesion protein that is important for attachment and stabilization of astrocytes in vitro, as well as their communication with the extracellular matrix in vivo and in vitro. The posttreatment time point of DIV7 was of particular interest because it coincides with the isoflurane-induced impairment in ASF formation (Fig. 2F). Isoflurane caused a significant decrease in the protein content of paxillin when measured

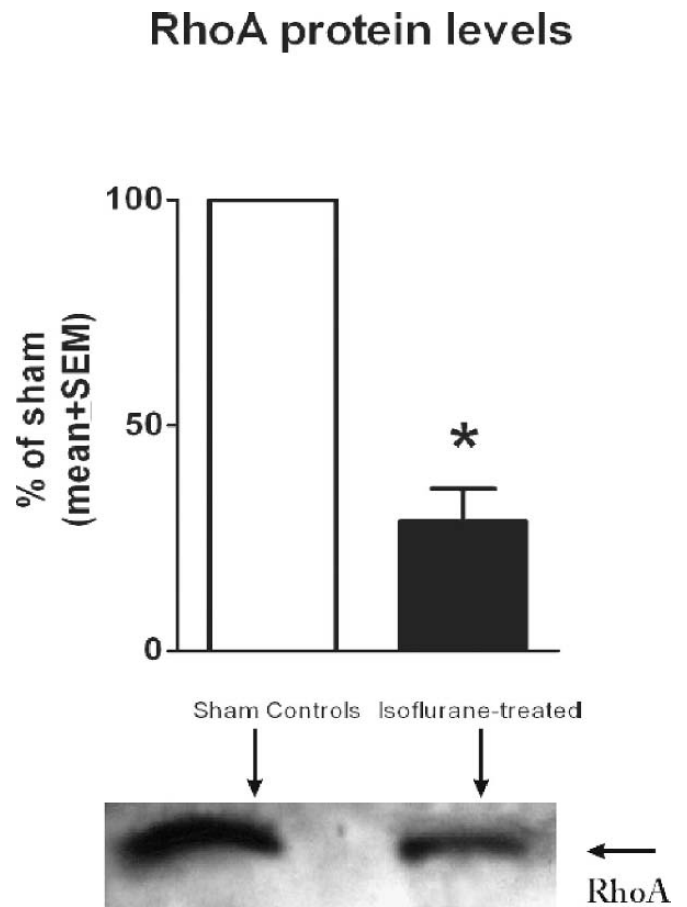


FIGURE 6. Isoflurane induces a decrease in levels of endogenous RhoA in immature primary astroglia. Isoflurane treatment at Day-In-Vitro 4 (DIV4) (3% for 24 hours) causes a decrease of approximately 75% in the protein content of endogenous RhoA when measured at DIV7 (2 days posttreatment; * $p < 0.01$; $n = 4$ per data point). Experimental cultures were compared with age-matched sham control cultures (noted as 100%). Corresponding representative Western blots are shown below the graph.

at DIV7 (Fig. 5). Paxillin levels in experimental astrocytes were approximately 2-fold lower than levels in sham controls (* $p < 0.005$; $n = 4$ per data point).

Isoflurane Modulates Protein Levels of Small GTPase, Rho A, and Its Downstream Effector MLC-P

To determine whether isoflurane-induced effects on the actin cytoskeleton are, at least in part, caused by modulation of the RhoA/MLC-P pathway, we measured the levels of RhoA at DIV7 in cultures treated with isoflurane or air at

FIGURE 4. Isoflurane has no effect on glial fibrillary acidic protein (GFAP), vimentin, or total actin protein content in immature primary astroglia. Isoflurane treatment at Day-In-Vitro 4 (DIV4) (3% for 24 hours) has no effect on the protein levels of GFAP, vimentin, or total actin when measured at DIV7 (2 days posttreatment). Experimental cultures were compared with age-matched sham control cultures (designated as 100%; $n = 4$ per data point). Corresponding representative Western blots are shown below the graph.

DIV4. RhoA levels were decreased by about 4-fold in experimental astrocytes versus controls ($*p < 0.01$, Fig. 6; $n = 4$ per data point). Furthermore, when the protein levels of total MLC were determined and compared with the protein levels of the activated (phosphorylated) form of MLC (MLC-P) at DIV7, we found that isoflurane treatment significantly down-regulated both the total protein level of MLC ($*p < 0.005$, $n = 5$ per data point; Fig. 7A) and its phosphorylated fraction (MLC-P) ($*p < 0.005$; Fig. 7B), while maintaining the MLC-P fraction (determined as the MLC-P/MLC + MLC-P ratio) roughly similar (control group, $49.89\% \pm 7.04\%$; experimental group, $52.89\% \pm 12.85\%$; Fig. 7C).

DISCUSSION

We have demonstrated that the volatile anesthetic isoflurane delays proper morphological differentiation and impairs the growth of immature astrocytes in primary culture by causing significant disturbances in 3 important factors of

astrocyte morphology and function: ASF formation, cytoskeletal organization, and paxillin content. Cytoskeletal reorganization was accompanied by significant downregulation of endogenous RhoA protein, a member of the Rho family of GTP-binding proteins, which controls ASF formation and, consequently, astroglia morphology, maturation, and growth. Isoflurane-induced RhoA-modulated disruption of actin cytoskeletal organization is, at least in part, mediated via the MLC signaling cascade (Fig. 8).

Our findings suggest that isoflurane causes significant impairment in morphological transformation during the early stages of astroglia maturation, as documented by the scarcity of well-developed ASF, as well as reduced branching and the undue presence of cortical actin in isoflurane-treated cells. Similar disturbances in actin cytoskeletal organization during the early stages of glial maturation have been shown to impair timely formation of a highly organized syncytial glial network that is crucially important in young brain development (27–31).

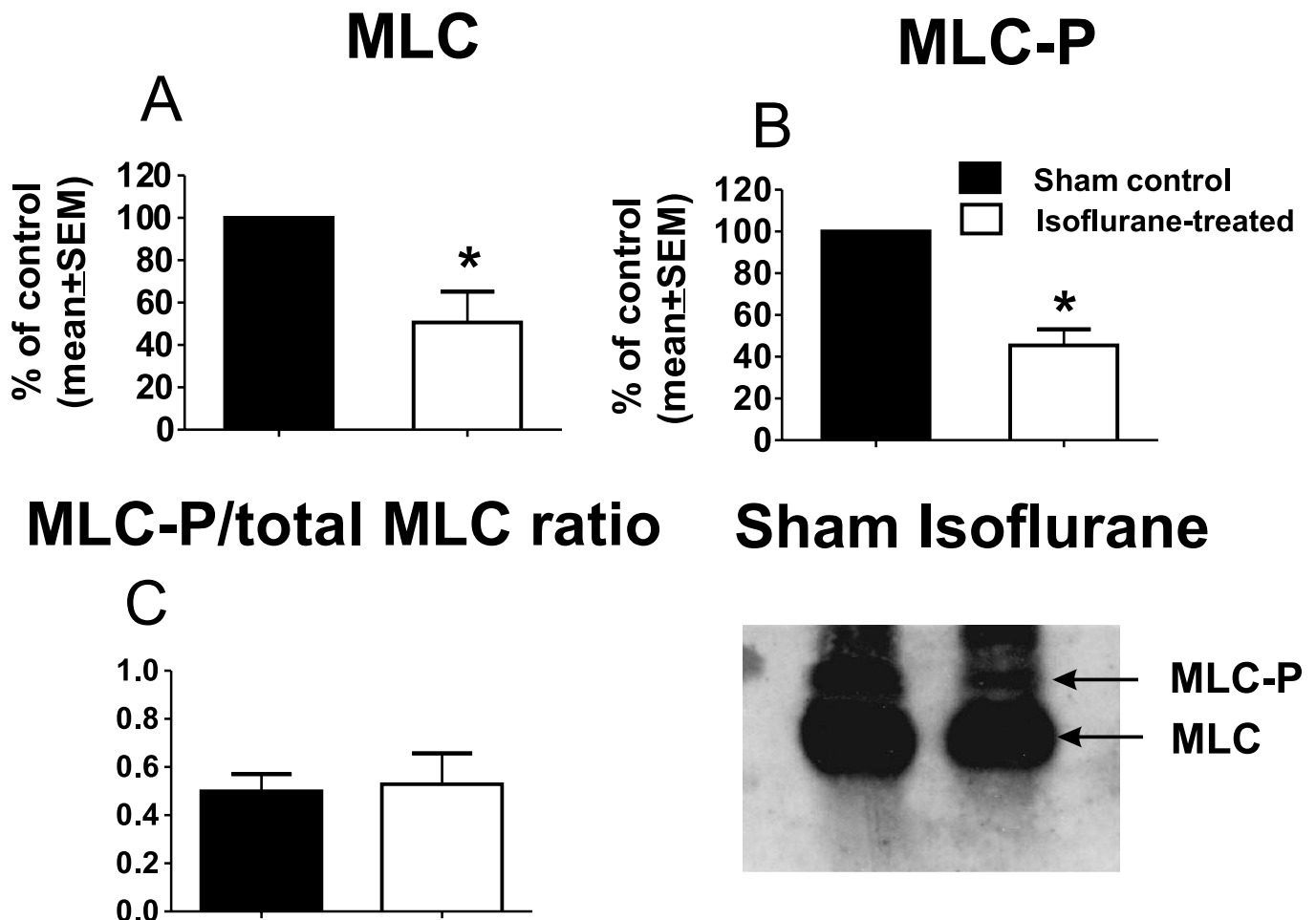


FIGURE 7. Isoflurane induces a decrease in protein levels of endogenous myosin light chain (MLC) and its activated (phosphorylated) form, MLC-P, in immature primary astroglia. **(A, B)** Isoflurane treatment at Day-In-Vitro 4 (DIV4) (3% for 24 hours) causes decreases of approximately 50% and 40% in the protein content of endogenous MLC **(A)** and its phosphorylated fraction (MLC-P) **(B)**, respectively, when measured at DIV7 (2 days posttreatment; $*p < 0.005$; $n = 5$ per data point). **(C)** The MLC-P fraction (MLC-P/MLC + MLC-P ratio) remained roughly similar (~50%) in sham control and experimental groups. Experimental cultures were compared with age-matched sham control cultures (noted as 100%). Corresponding representative Western blots are shown in the right panel.

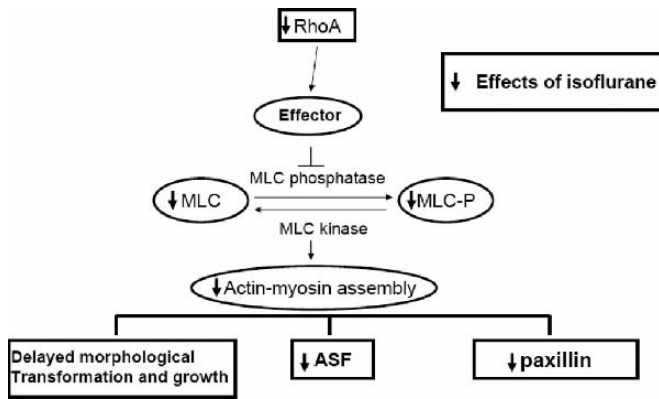


FIGURE 8. Isoflurane modulates key components of the RhoA signaling cascade. Isoflurane-induced actin cytoskeleton-mediated disturbances of glial morphological transformation and growth are associated with modulation of the RhoA/MLC-mediated cascade. Substantial downregulation of endogenous RhoA and myosin light chain/phosphorylated myosin light chain (MLC/MLC-P) coincides with significant downregulation of endogenous paxillin and disturbances in glial growth, morphological transformation, and the formation of actin stress fibers (ASFs).

Once the syncytial network has been formed, glia might be less vulnerable to exogenous insults. Our observation that isoflurane-induced impairment in actin morphology is likely age and maturation dependent is consistent with this concept, although it remains to be determined whether isoflurane can influence other important aspects of mature astrocyte function without affecting glial growth, morphology, and/or actin stress fiber formation. Although the causes of the age- and maturity-dependent vulnerability that we and others (21) have found are not fully understood, it is possible that differential susceptibility could be because the expression and properties of cell surface transporters and ion channels vary at different stages of astroglia maturity, thus making them more or less sensitive to certain toxic insults. For example, the coupling efficiency of calcium signaling (28, 29), chloride channel gating (27), and cell surface expression of some astrocyte glutamate transporters (e.g. GLAST and GLT-1) (29, 31) rely on proper cytoskeletal formation and the processes formation that promote glial growth, communication, and the formation of a tightly intertwined and woven glial syncytium. Therefore, we propose that isoflurane, by disrupting proper cytoskeletal actin organization, modulates a variety of glial cell surface transporters and ion channels in an age-dependant fashion. Further studies are needed to confirm this hypothesis.

The actin cytoskeleton, one of the major determinants of astrocyte morphology, motility, adhesion, and migration, undergoes extensive and constant sculpting to accommodate many demands of astroglial development (32). By polymerizing, G-actin forms filament bundles (F-actin), which become more densely organized in ASF running throughout the cytoplasm and glial processes as glia mature. Normally, ASFs are linked and anchored to the extracellular matrix through specific proteins, such as paxillin, that are localized at focal adhesion complexes. The formation of ASFs and focal adhesions must be finely balanced and precisely timed to allow proper devel-

opment, differentiation, and growth of developing astrocytes (15). Based on our findings, it seems that isoflurane disturbs this fine balance by downregulating paxillin levels and disorganizing ASFs.

During brain development, astroglia undergo morphological changes characteristic of extensive formation of cellular processes. That process relies on complex temporal changes in the relative presence and protein expression of vimentin and GFAP. It is becoming increasingly clear that the dynamic nature of intermediate filaments depends on the regulation of filament assembly and disassembly by phosphorylation of their head domains. Studies with reactive astrocytes lacking both GFAP and vimentin have shown that cytoskeletal bundle formation does not occur, indicating that the relationship between vimentin and GFAP is complex and highly intertwined (33). Although vimentin and GFAP lack enzymatic activity, they have an important part in maintaining the mechanical stability and shape of astrocytes; they also assist in the organization of the cytoplasm and organelles. Of particular relevance to this study is the finding that intermediate filaments contribute to astrocyte motility, which is essential to proper neuronal development. It seems that GFAP and vimentin expression during early stages of astrocyte development differ under in vitro and in vivo conditions (25, 26, 34). Our findings are consistent with the notion that a robust increase in GFAP expression from DIV4 until DIV15 (~4-fold) is accompanied by essentially unchanged expressions of vimentin. The reason for the different expression of these 2 crucial intermediates under in vivo and in vitro conditions remains elusive.

Not surprisingly, the actin cytoskeleton imbalance coincides with the greatest effect on glial growth. Thus, at 1 day (DIV6) and 2 days (DIV7) after isoflurane treatment, we found impaired glial growth and a significant decrease in the number of ASF-containing glial cells. Interestingly, although isoflurane seemed to disturb the spatial organization of the actin cytoskeleton, it had no effect on the total protein content of actin. In that respect, isoflurane mimics the effect of ethanol on developing glia. For example, Guasch et al (17) showed that cultured glia chronically exposed to physiologically relevant concentrations of ethanol have altered actin organization, shown as the formation of groups of bundles around the cell periphery (i.e. cortical actin), which gradually are reorganized into continuous actin rings. We found that although there was a clear presence of cortical actin in isoflurane-treated cells, the formation of cortical rings was not significant after an acute exposure to isoflurane (data not shown). It remains to be examined whether prolonged exposure to isoflurane results in the formation of actin rings similar to those that occur after chronic exposure to ethanol. It is noteworthy that although the number of glial cells displaying ASF was significantly reduced after isoflurane treatment at DIV6 and DIV7, not all astrocytes displayed actin reorganization, which suggests differential susceptibilities to the effects of isoflurane. Indeed, astroglia, especially immature ones, contain different subpopulations of astrocytes that display both functional and pharmacological heterogeneity (35, 36).

Our findings suggest involvement of the RhoA signaling pathway in isoflurane-induced actin alterations. Interestingly, earlier findings indicate that substantial downregulation

of endogenous RhoA protein often results in the impairment of RhoA function, especially in cases of chronic modulation (17). It remains to be determined whether acute exposure to isoflurane also affects Rho-GDI complex dissociation and/or impairs its binding to RhoA receptors on the effectors, especially in view of the profound (4-fold) downregulation of RhoA protein content.

RhoA activation is a complex phenomenon that requires interaction not only with other Rho GTPases (e.g. RhoE, Rac-1, and Cdc42), but also with a variety of effectors (e.g. ROCK-1 and PAK-1) (16, 37) that control downstream aspects of the pathway (especially MLC/MLC-P balance). Therefore, it remains to be determined whether isoflurane interferes at different and perhaps multiple levels of this signaling cascade. Interestingly, although chronic exposure to ethanol was found not to affect MLC-P (17), a RhoA downstream protein that is crucial for the linkage of actin-myosin fibers and, consequently, for ASF formation, we found that isoflurane treatment was detrimental not only to protein levels of endogenous MLC, but also to its activated form (MLC-P). Because the MLC-P fraction remained roughly unchanged as compared with the control condition, it is most likely that the effects of isoflurane on MLC-P are caused by downregulation of its substrate (MLC), which in turn results in significant reorganization of the actin cytoskeleton, impairment of ASF formation, and delay in glial morphological transformation indicative of slowed maturation.

Previous reports have shown that Rho-dependent actin reorganization, from stress fibers to cortical actin and actin rings as well as oval-type morphology, occurs in cells that are committed to die by apoptotic mechanisms (38, 39). In that sense, isoflurane-induced actin reorganization, cortical actin formation, and “rounded” morphological transformation combined with a reduction in paxillin could represent a series of initial steps in apoptotic activation. Based on our results, however, this is less likely because less than 4% of immature astrocytes die after isoflurane treatment, and a negligible number of isoflurane-treated astroglia have fragmented apoptotic nuclear morphology (unpublished observation).

It is becoming clear that astrocytes, by regulating neuronal migration, maturation, and synapse formation and sculpting, control every aspect of brain development (9, 10). By the end of synaptogenesis, mature astrocytes are highly coupled in a syncytial network that propagates calcium waves and modulates the function of synaptic circuits by releasing gliotransmitters, as well as by forming direct contact with developing neurons. This indicates that astrocytes actively mold neuronal circuits during development, which is contrary to the simplistic original view that the formation of synapses is an ability intrinsic to neurons. For example, in vitro studies in which neurons were cultured in the absence of the astrocytic feeding layer have shown little spontaneous synaptic activity compared with the high level of synaptic activity that occurs in neurons grown with the astrocytic feeding layer (10, 11).

Further studies have confirmed that the ability of astrocytes to increase synaptic activity is accounted for by a significant increase in synapse number, as well as synapse function, leading, in some in vitro systems, to a nearly 100-fold increase in synaptic activity (10). Although it remains to be established whether and how the isoflurane-induced impair-

ment of glial morphological transformation and growth observed in the present study may affect the function of neurons and the formation of synapses, our recent in vivo evidence suggests that an isoflurane-containing anesthesia cocktail, when administered at the peak of synaptogenesis, causes severe long-term impairment of synapse formation, which is manifested as a decrease in synapse number and an increase in redundant synapsing (8). Although this study did not examine the effects of anesthesia on immature glia, the fact that isoflurane impairs the development of astroglia in vitro raises the question of whether astroglia could be an important, although thus far neglected player, in the detrimental effects of general anesthetics on developing neurons.

In conclusion, our results demonstrate that isoflurane profoundly disrupts actin cytoskeleton organization and that these effects are accompanied by RhoA and MLC modulation. Isoflurane-induced downregulation of endogenous RhoA and MLC-P could be the triggering events in impairment of the morphological transformation of radial glial cells to more mature astrocytes and, therefore, could have detrimental functional consequences for developing glia. In view of the fact that astroglia are central to proper neuronal development, our study points, for the first time, toward the possibility that isoflurane-induced developmental neurotoxicity could be caused not only by a direct toxic effect on neurons, but also by isoflurane-induced actin cytoskeleton-mediated glial impairment.

ACKNOWLEDGMENTS

Drs Lunardi and Hucklenbruch contributed equally to cell culturing, isoflurane treatment, and generation of the data presented in Figure 3. The authors thank Hannelore Asmussen for technical assistance with primary glial cultures.

REFERENCES

1. Ikonomidou C, Bosch F, Miksa M, et al. Blockade of NMDA receptors and apoptotic neurodegeneration in the developing brain. *Science* 1999; 283:70–74
2. Ikonomidou C, Bittigau P, Ishimaru MJ, et al. Ethanol-induced apoptotic neurodegeneration and fetal alcohol syndrome. *Science* 2000;287:1056–60
3. Jevtovic-Todorovic V, Hartman RE, Izumi Y, et al. Early exposure to common anesthetic agents causes widespread neurodegeneration in the developing rat brain and persistent learning deficits. *J Neurosci* 2003;23: 876–82
4. Young C, Jevtovic-Todorovic V, Qin YQ, et al. Potential of ketamine and midazolam, individually or in combination, to induce apoptotic neurodegeneration in the infant mouse brain. *Br J Pharmacol* 2005;146: 189–97
5. Rizzi S, Carter LB, Ori C, et al. Clinical anesthesia causes permanent damage to the fetal guinea pig brain. *Brain Pathol* 2008;18:198–210
6. Slikker W Jr, Zou X, Hotchkiss CE, et al. Ketamine-induced neuronal cell death in the perinatal rhesus monkey. *Toxicol Sci* 2007;98:145–58
7. Pesić V, Milanović D, Tanić N, et al. Potential mechanism of cell death in the developing rat brain induced by propofol anesthesia. *Int J Dev Neurosci* 2009;27:279–87
8. Lunardi N, Ori C, Erisir A, et al. General anesthesia causes long-lasting disturbances in the ultrastructural and functional properties of developing synapses in young rats. *Neurotoxicity Res* 2010;17:179–88
9. Barres BA. The mystery and magic of glia: A perspective on their roles in health and disease. *Neuron* 2008;60:430–40
10. Ullian EM, Christopherson KS, Barres BA. Role for glia in synaptogenesis. *Glia* 2004;47:209–16
11. Pfrieger FW, Barres BA. Synaptic efficacy enhanced by glial cells in vitro. *Science* 1997;277:1684–87

12. Runquist M, Alonso G. GABAergic signaling mediates the morphological organization of astrocytes in the adult rat forebrain. *Glia* 2003;41:137–51
13. Fraser DD, Mudrick-Donnon LA, MacVicar BA. Astrocytic GABA receptors. *Glia* 1994;11:83–93
14. Franks NP. General anesthesia: From molecular targets to neuronal pathways of sleep and arousal. *Nat Rev Neurosci* 2008;9:370–86
15. Hall A. Rho GTPases and the actin cytoskeleton. *Science* 1998;279:509–14
16. Bishop AL, Hall A. Rho GTPases and their effector proteins. *Biochem J* 2000;348:241–55
17. Guasch RM, Tomas M, Miñambres R, et al. RhoA and lysophosphatidic acid are involved in the actin cytoskeleton reorganization of astrocytes exposed to ethanol. *J Neurosci Res* 2003;72:487–502
18. Miñambres R, Guasch RM, Perez-Aragó A, et al. The RhoA/ROCK-1/MLC pathway is involved in the ethanol-induced apoptosis by anoikis in astrocytes. *J Cell Sci* 2006;119:271–82
19. Goslin K, Asmussen H, Banker G. Rat hippocampal neurons in low-density culture. In: G. Banker and K. Goslin, eds. *Culturing Nerve Cells*. 2nd ed. Cambridge, MA: MIT Press, 1998;339–70
20. Heffron DS, Mandell JW. Opposing roles of ERK and p38 MAP kinases in FGF2-induced astroglial process extension. *Mol Cell Neurosci* 2005;28:779–90
21. Xu L, Chock VY, Yang EY, et al. Susceptibility to apoptosis varies with time in culture for murine neurons and astrocytes: Changes in gene expression and activity. *Neurol Res* 2004;26:632–43
22. Sall JW, Stratmann G, Leong J, et al. Isoflurane inhibits growth but does not cause cell death in hippocampal neural precursor cells grown in culture. *Anesthesiology* 2009;110:826–33
23. Stratmann G, Sall JW, May LD, et al. Isoflurane differentially affects neurogenesis and long-term neurocognitive function in 60-day-old and 7-day-old rats. *Anesthesiology* 2009;110:834–48
24. Weathersby PK, Homer LD. Solubility of inert gases in biological fluids and tissues: A review. *Undersea Biomed Res* 1980;7:277–96
25. Sancho-Tello M, Vallés S, Montoliu C, et al. Developmental pattern of GFAP and vimentin gene expression in rat brain and in radial glial cultures. *Glia* 1995;15:157–66
26. Meyer SA, Ingraham CA, McCarthy KD. Expression of vimentin by cultured astroglia and oligodendroglia. *J Neurosci Res* 1989;24:251–59
27. Lascola CD, Nelson DJ, Kraig RP. Cytoskeletal actin gates a CF channel in neocortical astrocytes. *J Neurosci* 1998;18:1679–92
28. Cotrina ML, Lin JH, Nedergaard M. Cytoskeletal assembly and ATP release regulate astrocytic calcium signaling. *J Neurosci* 1998;18:8794–804
29. Duan S, Anderson CM, Stein BA, et al. Glutamate induces rapid up-regulation of astrocyte glutamate transport and cell-surface expression of GLAST. *J Neurosci* 1999;19:10193–200
30. Sergeeva M, Ubl JJ, Reiser G. Disruption of actin cytoskeleton in cultured rat astrocytes suppresses ATP- and bradykinin-induced $[Ca^{2+}]_i$ oscillations by reducing the coupling efficiency between Ca^{2+} release, capacitative Ca^{2+} entry, and store refilling. *Neuroscience* 2000;97:765–69
31. Sullivan SM, Lee A, Bjorkman T, et al. Cytoskeletal anchoring of GLAST determines susceptibility to brain damage: An identified role for GFAP. *J Biol Chem* 2007;282:29414–22
32. John GR, Chen L, Rivieccio MA, et al. Interleukin-1beta induces a reactive astroglial phenotype via deactivation of the Rho GTPase-Rock axis. *J Neurosci* 2004;24:2837–45
33. Pekny M, Wilhelmsson U, Bogestål YR, et al. The role of astrocytes and complement system in neural plasticity. *Int Rev Neurobiol* 2007;82:95–111
34. Sáez R, Burgal M, Renau-Piqueras J, et al. Evolution of several cytoskeletal proteins of astrocytes in primary culture: Effect of prenatal alcohol exposure. *Neurochem Res* 1991;16:737–47
35. Montoliu C, Sancho-Tello M, Azorin I, et al. Ethanol increases cytochrome P4502E1 and induces oxidative stress in astrocytes. *J Neurochem* 1995;65:2561–70
36. Climent E, Sancho-Tello M, Miñana R, et al. Astrocytes in culture express the full-length Trk-B receptor and respond to brain derived neurotrophic factor by changing intracellular calcium levels: Effect of ethanol exposure in rats. *Neurosci Lett* 2000;288:53–56
37. Moorman JP, Luu D, Wickham J, et al. A balance of signaling by Rho family small GTPases RhoA, Rac1 and Cdc42 coordinates cytoskeletal morphology but not cell survival. *Oncogene* 1999;18:47–57
38. Rosenblatt J, Raff MC, Cramer LP. An epithelial cell destined for apoptosis signals its neighbors to extrude it by an actin- and myosin-dependent mechanism. *Curr Biol* 2001;11:1847–57
39. Mills JC, Stone NL, Pittman RN. Extranuclear apoptosis. The role of the cytoplasm in the execution phase. *J Cell Biol* 1999;146:703–8